

Comparative electrodeposition of Ni–Co nanoparticles on carbon materials and their efficiency in electrochemical oxidation of glucose

Adina Arvinte¹ · Florica Doroftei¹ · Mariana Pinteala¹

Received: 20 July 2015 / Accepted: 8 December 2015 / Published online: 28 December 2015
© Springer Science+Business Media Dordrecht 2015

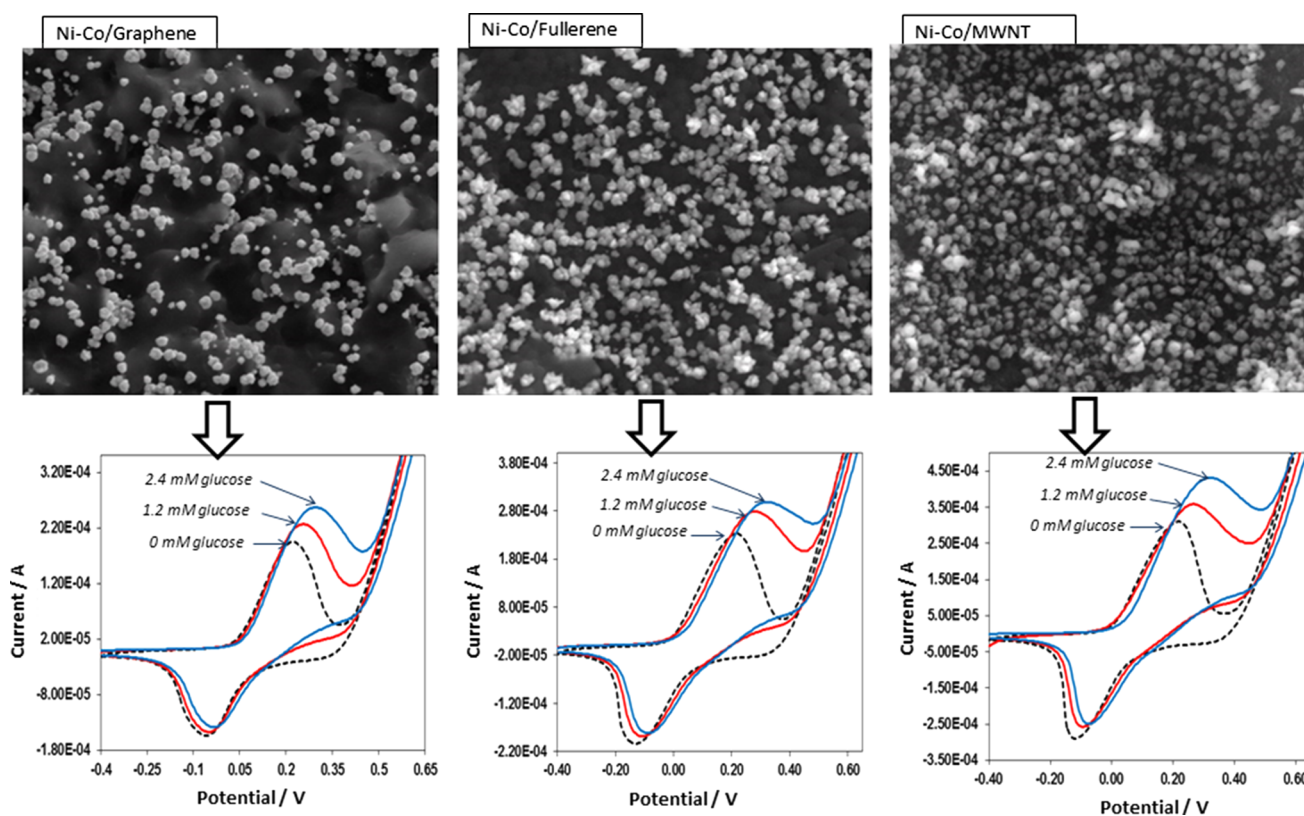
Abstract The use of carbon materials (graphene, multi-wall carbon nanotubes, and fullerene) as templates for comparative electrodeposition of Ni–Co nanostructures is described. Operating conditions and parameters were found to influence in a challenging manner the morphology and electrochemical activity of the electrodeposited Ni–Co nanoparticles. The electrocatalytic properties of Ni–Co/carbon material-modified electrode toward the

glucose oxidation were analyzed via cyclic voltammetry and amperometry. The studies showed that Ni–Co/MWNT electrode displayed the highest electrocatalytic activity, attributed to the high density of Ni–Co nanoparticles deposited on the carbon nanotubes support. A low detection limit of 1.8 μM glucose with a good sensitivity of 1868 $\mu\text{A mM}^{-1} \text{cm}^{-2}$ was obtained for electrochemical detection at Ni–Co deposited on MWNT.

✉ Adina Arvinte
adina.arvinte@icmpp.ro

¹ “Petru Poni” Institute of Macromolecular Chemistry, Centre of Advanced Research in Nanobioconjugates and Biopolymers, Grigore Ghica Voda Alley 41A, 700487 Iasi, Romania

Graphical Abstract



Keywords Ni–Co nanoparticles · Electrodeposition · Carbon nanomaterials · Glucose

1 Introduction

Additional modification of carbon nanomaterials, for example, with metal or metal oxide nanoparticles, may bring in great benefits for electrochemical sensing application. The larger specific surface areas, higher electrocatalytic activity and conductivity enable the construction of carbon–metal nanomaterials-based electrochemical sensors with high sensitivity and stability for different chemical/biological species detection. Numerous studies have shown that carbon nanomaterials decorated or in combination with metal nanoparticles such as Au [1, 2], Ag [3], Pt [4, 5], Ni [6, 7], Co [8], Cu [9, 10] can improve the sensitivity and response time of electrochemical sensors towards the sensing of glucose. Alloys and bimetallic-based electrodes were widely used as non-enzymatic glucose sensors due to their highly desirable electronic and catalytic properties [11–17].

Considerable focus has been on methods that allow controlling the particle size and distribution as there is

evidence that size, quantity, and agglomeration directly affect the electrochemical properties of the nanoparticles and nanocomposite [18, 19]. Among physical, chemical, and electrochemical methods developed to synthesize metal nanoparticles–carbon nanocomposites, electrochemical deposition has been proven as a powerful tool for the fabrication of inorganic nanoparticles and their relative carbon–metal nanocomposites due to their advantages: (i) easy control of size distributions and densities of metal nanoparticles by tuning the concentration of metal precursors and the electrochemical deposition parameters such as applied potential and deposition time; (ii) large-scale synthesis; (iii) short-term formation [18, 20, 21]. The electrochemical deposition method involves simple reduction of metal cations on selected substrates from an electrolyte solution due to the application of a suitable potential (the electrochemical driving force) and enables effective control of nucleation and growth procedure in material synthesis.

Ni–Co alloy electrodeposition has been patented by many research groups [22–27] and most of the procedures involve pulsed electrodeposition process and are aimed for applications such as supercapacitor electrodes for energy storage.

Concerning scientific publications, the mechanism, morphology, composition, microstructure, and life time of electrodeposited Ni–Co alloys have been intensively investigated [19, 28–32]. Likewise, applications of Ni–Co alloy as electrocatalyst for the oxygen and hydrogen evolution reactions is well represented in the literature [33–36], but research of the electrocatalytic properties of differently electrodeposited Ni–Co alloy towards glucose detection was rarely reported so far. Recently, Wolfart et al. [37] reported electrochemical deposition of nickel/cobalt alloys onto platinum and ITO electrodes, investigating different Ni/Co ratio and different deposition time in order to find the best electrode modification related to the best electrocatalytic behavior towards glucose. In that case, the obtained sensor showed even a lower sensitivity and LOD than those obtained by our group when using NiCo oxide in connection with CNT [38].

In the present work, comparative modification of electrodes through the electrochemical deposition of nickel–cobalt alloy nanoparticles onto carbonic materials is evaluated. Optimizing the deposition parameters and conditions enables to effectively control the morphology of bimetallic nanostructures, thus providing a great opportunity to improve their electrochemical properties.

The formation and electrochemistry of Ni–Co nanoparticles at the electrode surface as well as their variations with different electrodeposition conditions have been determined by cyclic voltammetry (CV). The changes in chemical composition and morphology of the nanoparticles-modified electrode surface as a function of the applied potential and cyclic number in the electrodeposition process has been studied by scanning electron microscopy technique (SEM), including microanalysis by energy dispersive X-ray method (EDX).

We have extended those studies to the target deposition of Ni–Co nanoparticles on different carbonaceous materials such as graphene, carbon nanotubes, and fullerene, from the same structural family but having different surface area, and probably presenting different active sites for nucleation processes. Graphene, a single-atom-thick layer of sp^2 carbon atoms densely packed into a two-dimensional (2D) honeycomb lattice, can be viewed as the basic building block for carbon materials of all other dimensionalities, such as 0D fullerene, 1D nanotubes. Carbon nanomaterials, especially graphene, fullerene, and carbon nanotubes are very promising candidates for materials engineering and controlled functionalization for the development of various electroanalytical applications.

The electrocatalytic activity of the Ni–Co nanoparticles deposited on graphene, carbon nanotubes, and fullerene was comparatively assessed by voltammetry and amperometry towards the glucose oxidation, corroborated with

SEM images, demonstrating the enhanced analytical response of modified electrodes with MWNT used as support materials for electrodeposited nanoparticles.

2 Experimental

2.1 Reagents

Nickel(II) chloride anhydrous 98 % and Cobalt(II) chloride anhydrous 97 %, KCl, KOH, dimethylformamide (DMF) were supplied by Sigma–Aldrich (www.sigmaaldrich.com). Graphene nanopowder (8 mm flakes) were purchased from Graphene Laboratories Inc. USA (<https://graphene-supermarket.com>) and Fullerene C60 99+ % from MER Corporation (<http://www.mercorp.com>). Multiwall carbon nanotubes (MWNT, 6–13 nm diameters and 2.5–20 μ m length, 99.8 % purity) were purchased from Sigma–Aldrich and used as received, without any further purification.

2.2 Apparatus and methods

Cyclic voltammetry for the deposition of Ni–Co coatings was performed using a potentiostat/galvanostat Autolab model PGSTAT302 N from ECO CHEMIE Utrecht, The Netherlands and a three-electrode system with a planar configuration of a screen-printed electrode (SPE), fabricated and purchased from Biosensor Laboratory, University of Florence, Italy. The working carbon-based electrode with a disk shape of 3 mm diameter, and the silver reference and carbon counter electrode were symmetrically disposed around working electrode. The deposition electrolyte solution was prepared according to the metal ion Ni/Co ratio of 1:1 using stock solutions of 20 mM $NiCl_2$ and 20 mM $CoCl_2$ in 20 mM KCl. This molar ratio has been chosen based on previous studies [38] where nickel–cobalt-mixed oxide with a linear formula (NiO) (CoO) 1:1 (provided by Sigma–Aldrich) and composited with MWNT was investigated for the electrocatalytic oxidation of carbohydrates, providing thus a point of comparison.

Cyclic voltammetry and amperometry methods were used to investigate the electrochemical properties of the deposited Ni–Co nanoparticles and to study the electrocatalytic measurements of glucose in 0.1 M KOH electrolyte solution. The potential range for CV was mentioned for each experiment (vs. Ag/AgCl). Amperometric assays were performed at constant applied potential of +0.3 V versus Ag/AgCl in 0.1 M KOH under continuous stirring.

The micrographs of the coatings were performed with Quanta 200-FEI scanning electron microscope and the ratio of Ni/Co was measured by energy dispersive spectrum (EDX) affiliated to SEM, using area mapping.

2.3 Modification of the electrode

To obtain graphene-modified electrode, 1 μL suspension of 2 mg mL^{-1} graphene in DMF was placed onto the working area of the screen-printed electrode and allowed to dry 24 h at room temperature. Next, a drop of 200 μL bath solution of 10 mM NiCl_2 and 10 mM CoCl_2 in 20 mM KCl was placed onto the graphene-modified electrode covering the whole electrode area and the potential was swept in a mentioned range, at 50 mV s^{-1} scan rate for a certain scan number. After electrodeposition, the electrode was rinsed with distilled water, dried at room temperature for 1 h, and ready to be used for further assays. The same procedure was used for MWNT and fullerene-based electrodes.

3 Results and discussion

3.1 Characterization of Ni and Co nucleation on graphene-modified electrode

In order to characterize the nucleation process and to obtain information about the reduction potential of Ni and Co, and therefore the potentials at which the metal can be electrodeposited, individual depositions of nickel and cobalt, from solutions of 10 mM concentration, were studied prior to codeposition.

Figure 1 illustrates cyclic voltammograms for NiCl_2 and CoCl_2 individual electrodeposition at a graphene-modified electrode. The first scan contains a characteristic “nucleation loop” in the cathodic range which indicates the three-dimensional nucleation of Ni deposits, respectively Co deposits [21, 39]. After the first scan, the concentration of electrochemically active positive ions adjacent to the electrode, especially in the double layer, will decrease sharply, explaining the significant decrease of cathodic

current for subsequent scans (not shown in figure). It is noticeable that the electrodeposition of Ni and Co ions from individual solution initiates at exactly the same potential (-0.95 V), which means that the number of instantly formed nuclei should be almost similar. The difference is in the anodic range, where the stripping of cobalt occurs around -0.2 V potential, while the anodic stripping peak for nickel on the return scan is fairly absent on the verified range. These observations indicate that the stripping process is different and that all the Ni nuclei remain on the graphene surface and the subsequent growth occurs predominantly at the existing nucleation sites. In the case of cobalt, the anodic stripping peak at -0.2 V indicates that a part of Co nuclei might be expelled from the electrode surface and the growth of the particles might be slowed down. This assumption is confirmed by the SEM images presented in Fig. 2.

The morphologies of the modified metal/graphene electrodes were characterized by SEM as depicted in Fig. 2. The image of Ni/graphene electrode revealed that Ni nanoparticles with a homogeneous grain size (of about 300 nm) were uniformly deposited on the graphene surface. When Co nanoparticles were grown on the electrode surface, the morphology shows that the deposited agglomerates were smaller and less homogeneous, with an average size of 100 nm. Also, smaller clusters, typically of 50 nm, between the agglomerates can be observed.

When Ni and Co were codeposited from a mixture containing 10 mM NiCl_2 and 10 mM CoCl_2 , the cyclic voltammogram of electrodeposition exhibited the same general features: in the cathodic branch a nucleation loop is recorded indicating the concomitant deposition of Ni and Co, the onset potential of deposition is not shifted to more negative nor positive values compared to their individual deposition, and the deposition current density gets greater (Fig. 3a). The stripping process is different: for the first

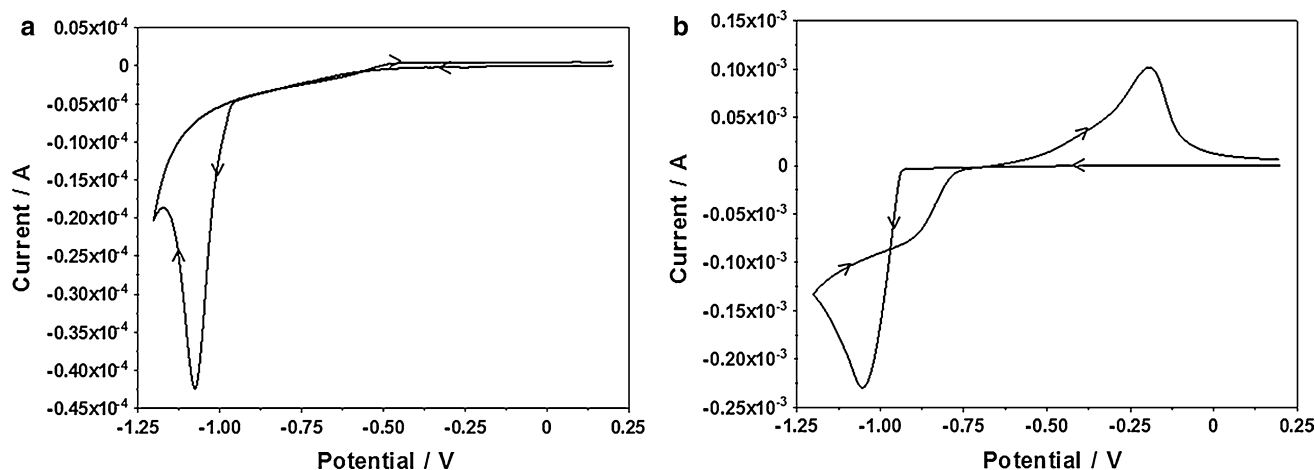


Fig. 1 Cyclic voltammetry of 10 mM NiCl_2 (a) and CoCl_2 (b) solutions in 20 mM KCl at graphene-modified electrodes; scan rate 50 mV s^{-1}

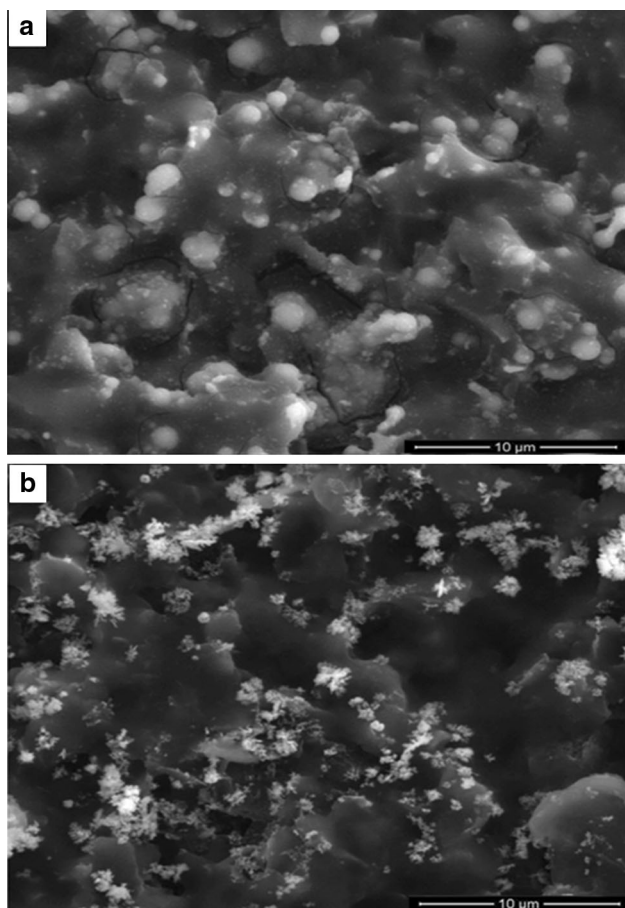


Fig. 2 Morphology of electrodeposited **a** Ni and **b** Co species onto graphene-modified electrodes. Deposition conditions: 50 mV s⁻¹, 25 scans (0.2 to -1.2 V)

scan, no anodic stripping peak could be seen (solid line) indicating that the initial formed nuclei will remain on the electrode surface, but for subsequent scans the stripping peak current is increasing with the cyclic number

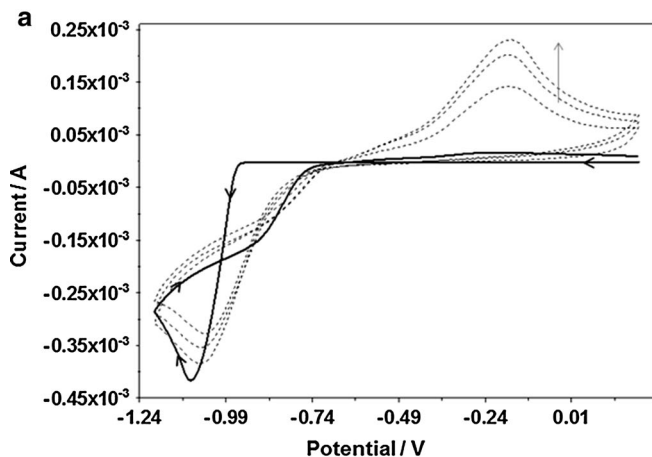
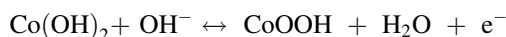


Fig. 3 a Electrochemical codeposition of Ni-Co from 10 mM NiCl₂ and 10 mM CoCl₂ in 20 mM KCl; first scan (solid line) and subsequent scans (dotted lines). Deposition conditions: 50 mV s⁻¹,

indicating a partial expulsion of cobalt from the surface (dotted lines). A higher percentage of Ni loading compared to Co loading is confirmed by EDX data (Fig. 4), endorsing the partial expulsion of cobalt from the surface of the electrode.

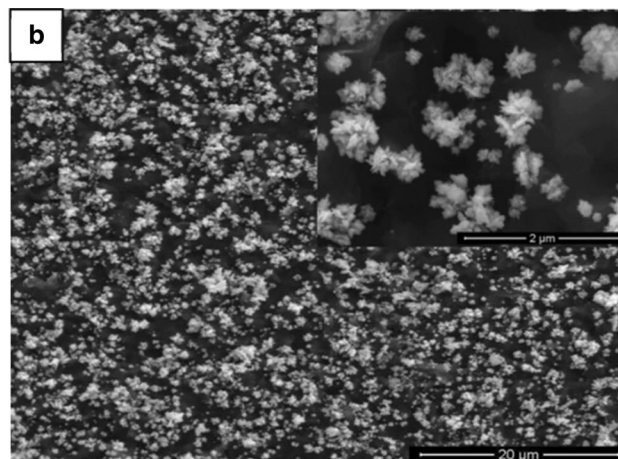
The differences in cyclic voltammograms of codeposition should account for the different morphology of the Ni-Co deposits which are confirmed by the following SEM observations. From Fig. 3b, grain-shaped nanoparticles of different sizes of 150–200 nm, uniformly distributed on the electrode surface could be observed. It is worthy to note that the density of Ni-Co nanoparticles on graphene increased comparing with the individual Co or Ni nanoparticles deposition. The formation of clusters can also be observed in the inset of Fig. 3b.

The electrochemical activity of as-prepared Ni/Graphene, Co/Graphene, and Ni-Co/Graphene-modified electrodes was investigated by CV technique in 0.1 M KOH aqueous solution (Fig. 5). In both cases of Ni and Co deposits, the redox peaks could be attributed to the redox transitions Ni²⁺/Ni³⁺ and Co²⁺/Co³⁺ as follows:



In accordance with EDX data, the higher peaks current of the Ni deposits compared to Co peaks current indicate a higher Ni loading deposited at the involved potential range. The formal potential estimated as midpoint of voltammetric reduction and oxidation peak potentials is about -0.03 V for Co and 0.24 V for Ni, with a separation between peak potentials ($\Delta E_p = E_{pa} - E_{pc}$) of 0.25 V for Co deposition and 0.3 V for Ni deposition as calculated from the corresponding cyclic voltammograms.

When Ni and Co are deposited together, their specific redox peaks are overlapping giving rise to a couple of



25 scans (0.2 to -1.2 V). **b** Morphology of Ni-Co deposited onto graphene-modified electrode. *Inset*: SEM image of Ni-Co with high magnification

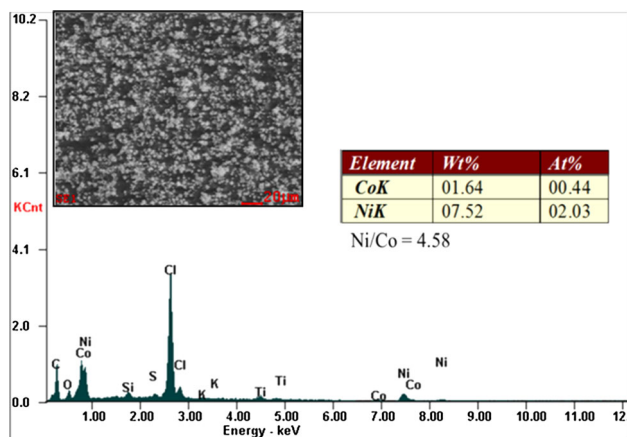


Fig. 4 EDX analyses of the surface of graphene-modified electrode after electrodeposition of Ni–Co, using deposition conditions as in Fig. 2. Inset: region of modified electrode used for EDX analysis

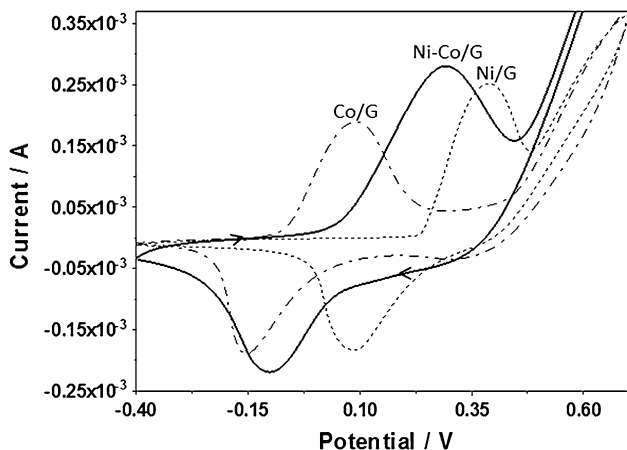


Fig. 5 Cyclic voltammetry of Ni/Graphene, Co/Graphene, and Ni–Co/Graphene-modified electrodes in 0.1 M KOH; scan rate: 50 mV s⁻¹

reinforced redox peaks at a formal potential shifted at 0.098 V versus Ag/AgCl, with a peak-to-peak separation of 0.39 V. Furthermore, the shapes of anodic and cathodic peaks were nearly symmetric, and the heights of reduction and oxidation peaks are the same. Likewise, the incorporation of Co into the Ni structure is presented in literature to lead a significant improvement in the electrochemical properties of nickel hydroxide, shifting the Ni²⁺/Ni³⁺ redox process to cathodic potentials and increasing the electronic transfer and the reversibility of the system [40, 41].

3.2 Influence of deposition potential range

The key properties of the metal nanoparticles involved in electrochemical sensing are the size and number density of nanoparticles on the surface of the electrode [42]. Some of

these properties can be controlled by careful choice of the applied potential as the driving force of nucleation, and duration of the applied potential, respectively scanning number. In order to maximize the particle size monodispersity it is necessary that the electrodeposition proceed via instantaneous nucleation, so that all nanoparticles are growing for the same amount of time, from the beginning of the experiment. In addition, the rate of growth must be limited so that the coupling of diffusion zones is kept at a minimum [43–46]. Therefore, finding a balance between large nucleation overpotential and a small overpotential for particle growth is crucial.

The possibility to control the nucleation and growth dynamics through the applied potential was investigated for the electrodeposition of Ni–Co nanoparticles from mixture containing 10 mM NiCl₂ and 10 mM CoCl₂ in KCl 20 mM. Figure 6a–d shows a series of current–voltage curves run for different potential windows. To conclude about the nucleation process, only the first scan from a set of 25 was depicted and presented comparatively in the figure. For curves a and b, the potential is swept from an initial positive value of 0.6 V, respectively 0.2 V, where no metal is deposited on the electrode surface, to –1.2 V. The characteristic shape of the curves confirms the occurrence of nucleation and growth processes in the system which is in agreement with the nucleation loop observed. As the potential scan direction was reversed, a characteristic anodic stripping peak was observed with different intensity depending on the final positive potential.

As it is expected to have an instantaneous nucleation mode at more negative potential [46], for curves c and d, the potential is swept to a more negative value (–1.3 V) and then reversed till –0.1 V, respectively –0.3 V, where the anodic stripping is partially or even totally avoided.

The effect of deposition potential range on the morphology of obtained Ni–Co particles is presented in Fig. 6 e–h. The synthesized metal nanoparticles are homogeneously dispersed on the graphene support, excepting the case of Fig. 6e where severe agglomeration occurred, which indicate that the anodic stripping process also influenced the growth of the particles, determining their size. Deposition at more cathodic potentials resulted in the increase of Ni–Co population density (Fig. 6g, h). Concomitantly, since the anodic stripping process is restricted, the nanoparticles are significantly smaller, with a mean diameter of approximately 100 nm and homogeneously dispersed (inset of Fig. 6h).

The voltammetric behavior of the Ni–Co nanoparticles deposited on graphene-modified electrode by cycling on different potential range has been evaluated in 0.1 M KOH solution and is shown in Fig. 7. The results partially correlated well with SEM data as the redox peak currents increase with decreasing the nanoparticles size and the

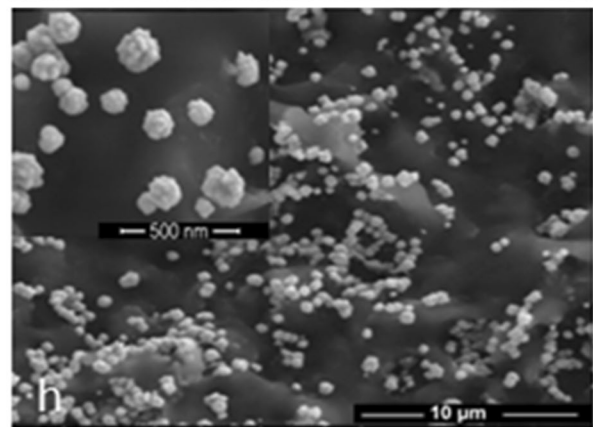
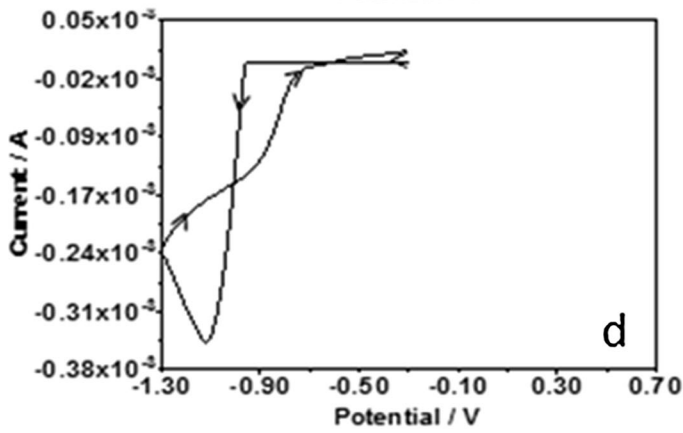
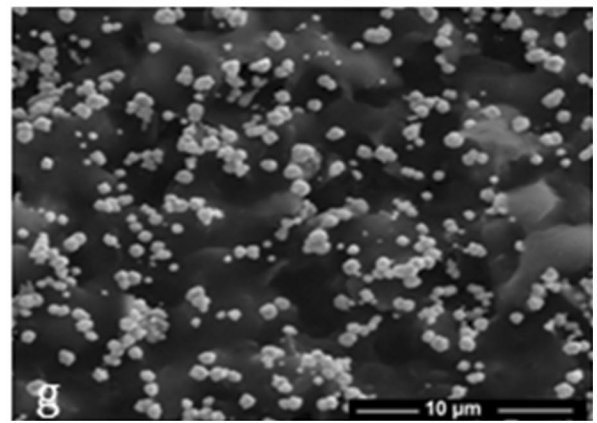
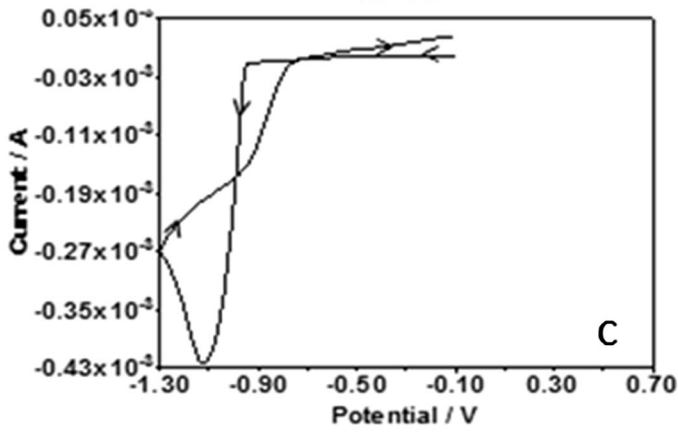
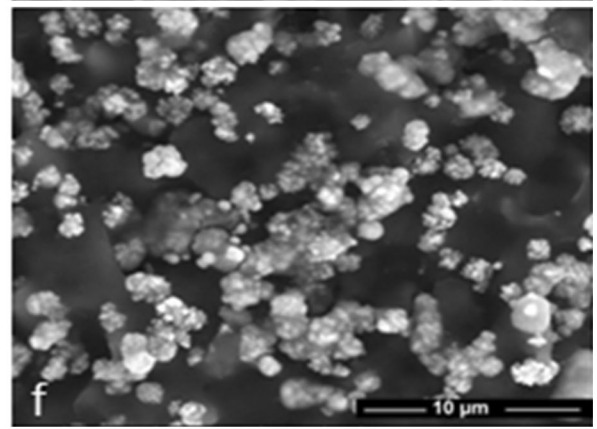
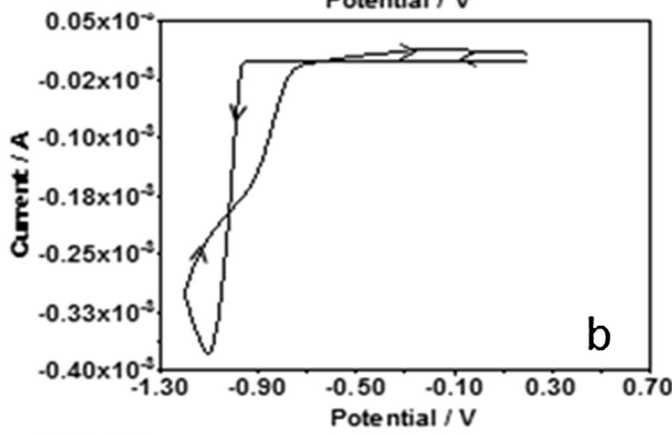
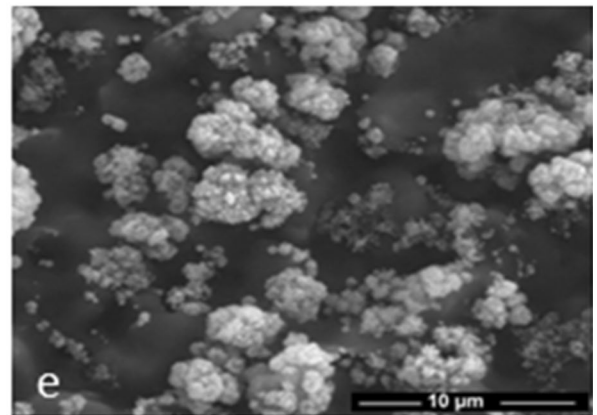
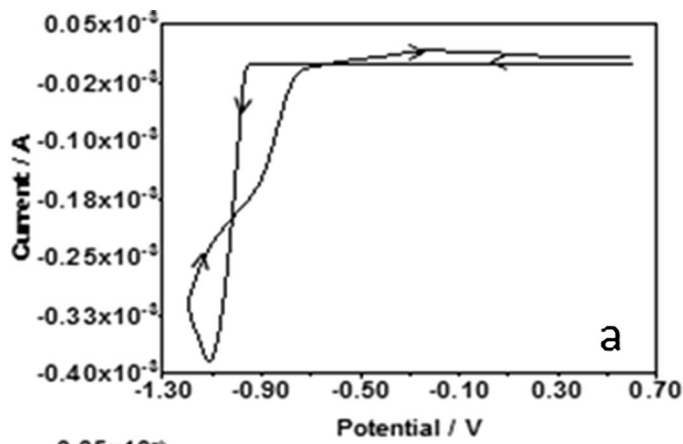


Fig. 6 Initial scan for Ni–Co electrodeposition on graphene on different potential ranges: **a** 0.6 to -1.2 V, **b** 0.2 to -1.2 V, **c** -0.1 to -1.3 V, and **d** -0.3 to -1.3 V and corresponding SEM images of modified electrode surfaces **e–h** deposition conditions: 50 mV s^{-1} , from 10 mM NiCl_2 and 10 mM CoCl_2 in 20 mM KCl

increase of their number. Surprisingly, the peak currents were lower for Ni–Co deposited in the range -0.3 to -1.3 V (Fig. 7 curve d'), even though the particles are smaller.

Several reports in the literature have shown a strong correlation between particle size and catalytic activities, indicating an increase of catalytic activity with the decrease of the particle size [47, 48]. In contrast to these results, also there are papers reporting the decrease of redox current densities or catalytic activity for decreasing particle sizes [49, 50], for example, S. Yu et al. [42] reported the size effect of Ni nanoparticles for the oxidation of glucose observing the highest response to glucose for Ni nanoparticles with intermediary size among the tested samples.

The Ni/Co ratio in the surface-deposited structures corresponding to Fig. 6 e–h was measured by EDX and were found to be 5.44, 4.58, 4.01, and 3.68, which are greater than that in the starting electrolyte solution (Ni/Co: 1/1). The results show that the deposition of Ni–Co is an anomalous codeposition, since the ratio of Ni/Co in the surface deposits is not in accordance with the starting ratio in the electrolyte solution. Ni is enriched within the Ni–Co alloys and this result does not agree with other data from literature describing the anomalous codeposition in which Co is preponderant in the alloy deposits [51–53]. This phenomenon could be explained by the influence of the stripping process of Co which occurs in the CV technique

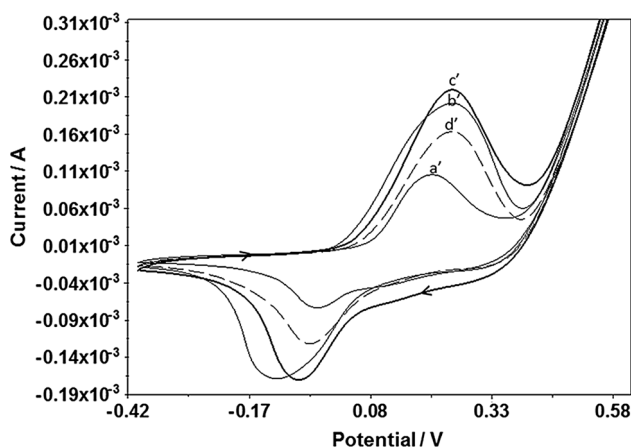


Fig. 7 Electrochemical behavior of Ni–Co/graphene electrodes in 0.1 M KOH , scan rate 50 mV s^{-1} . Ni–Co nanoparticles deposited according to conditions presented in Fig. 6a–d

(even though in low percentage when the scanning potential is stopped at less positive value) compared to potentiostatic deposition at static negative potential involved by other authors describing the higher loading of Co in the coatings. Although many attempts have been made to explain the anomalous codeposition of alloys, there is still no universally accepted theory [53].

3.3 Influence of deposition scanning number (cycling time)

To optimize the method and conditions for the production of high density, low size, and monodisperse Ni–Co nanoparticles, influence of the number of potential scanning was evaluated. Since agglomerated metallic particles are not favorable for electrochemical reactions, the following discussion is mainly focused on Ni–Co nanoparticles obtained by cycling the potential between -0.1 and -1.3 V corresponding to Figs. 6c, 7c'. To determine the suitable deposition duration, the redox behavior of Ni–Co at different electrodes prepared with different deposition scanning number is studied using CV in 0.1 M KOH (Fig. 8). The anodic peak current considerably increases with the deposition cycling time until 15 scans. It is expected that the total amount of deposited Ni–Co at graphene surface increases, explaining the enhancement of surface electrochemical activity.

With further increase of the deposition cycling time to 20 or 25 scans, the oxidation peak current of Ni–Co oxidation increases gradually, accompanied by a non-uniform increase of the reduction peak current. This might be due to the growth of the already existent particles accompanied by nucleation of newly formed small nanoparticles.

Further increase of the deposition to 30 scans results in an excessive deposition causing the aggregation of nanoparticles, thickening of the composite film, which

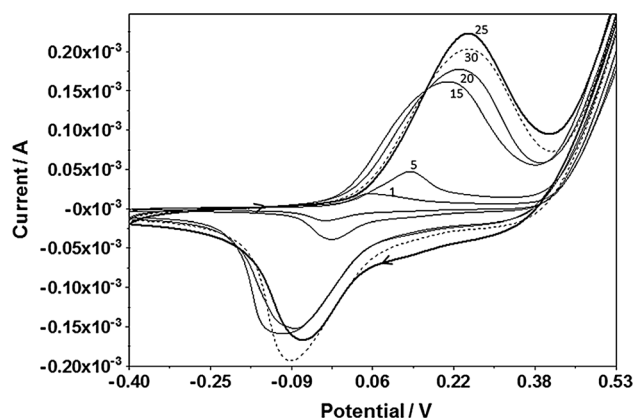


Fig. 8 Electrochemical behavior of Ni–Co/graphene-modified electrodes in 0.1 M KOH , scan rate 50 mV s^{-1} . Ni–Co nanoparticles deposited by 1, 5, 15, 20, 25, and 30 scans number

hinders the electronic transfer. This phenomenon explains thus the smaller oxidation peak current corresponding to this Ni–Co deposit from Fig. 8.

In order to better visualize the morphology of Ni–Co nanoparticles in the earlier stages of development, the SEM examination was performed for all the tested number of potential scanning. Figure 9 shows the SEM images of the Ni–Co samples after 1 scan, 5, 15, 20, 25, and 30 scans involved in the electrodeposition process. Uniformly distributed nanoparticles can be clearly observed, and the size of these nanoparticles increases as the deposition duration, respectively scanning the potential increases. Nanoparticles as small as 30 nm for 1 scan and as big as 200 nm for 25 scans can be homogeneously deposited on the graphene surface.

In the initial stage of electrodeposition, both nickel and cobalt nucleation occur at the most active energy sites of

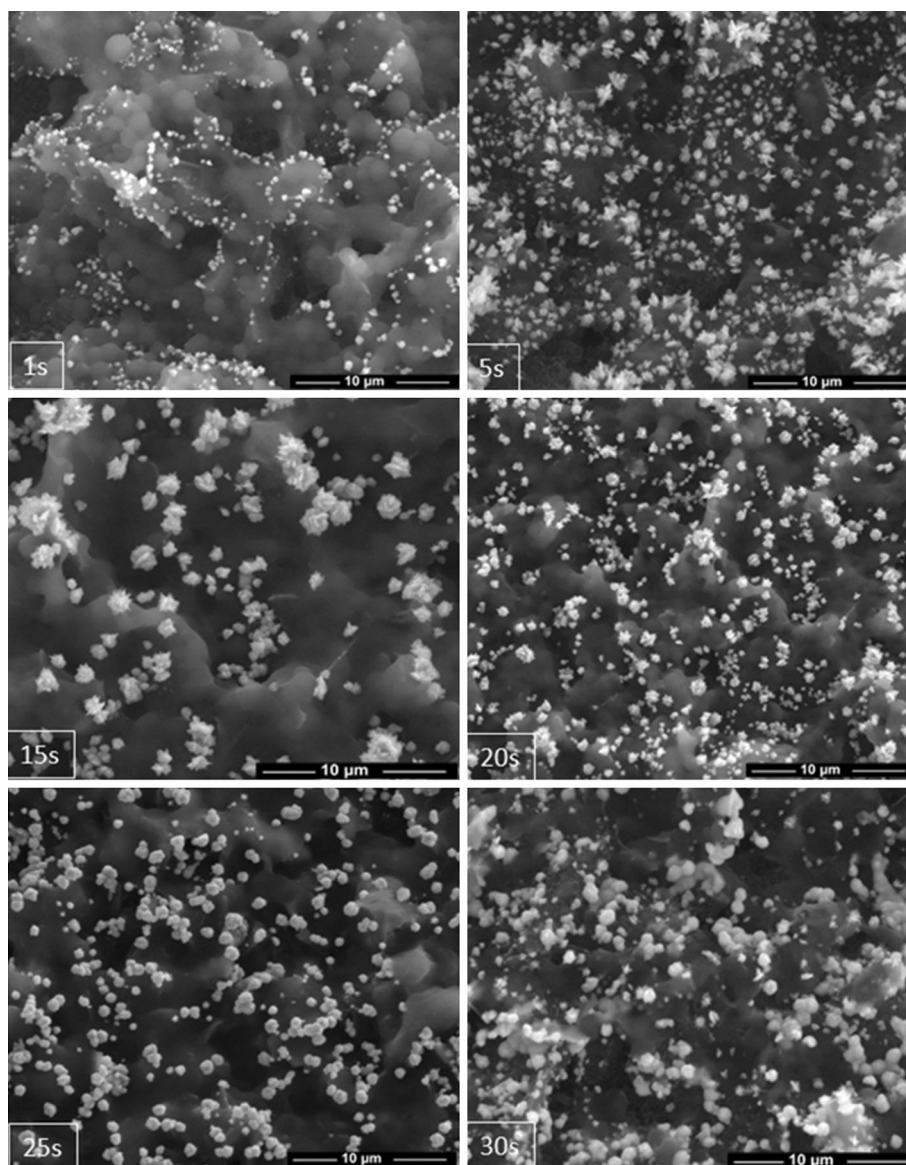
the electrode surface [54, 55]. In the growth process, due to the effect of current density distribution, further nickel and cobalt nucleation occur at top of groups of nickel and cobalt grain agglomerates.

The grain sizes grow large with the increase of cycling times. After the first scan, the grains are small but big enough to be identified clearly. When cyclic times reach 25 or 30 scans, the grains are large and the size is about 200 nm. It is also observed that the Co weight percent in the deposits increases significantly as the cycling times increases.

3.4 Comparative deposition of Ni–Co on graphene, CNT, and fullerene

Besides the preparation process with the involved parameters, Ni–Co particles size, number, and distribution can be

Fig. 9 SEM images of the Ni–Co nanoparticles deposited on the graphene electrode for 1 scan, 5, 15, 20, 25, and 30 scans on the -0.1 to -1.3 V potential range; scan rate 50 mV s^{-1}



influenced by the nature of the carbon nanomaterial used as support. When used as substrate, carbon nanomaterials achieve three essential roles: (1) to support the Ni–Co growth during the electrodeposition process, (2) to provide the active sites where the nucleation will proceed, and (3) to enhance the electronic transfer between the Ni–Co nanoparticles and the electrode in the sensing process. To exploit the best electrochemical activities from Ni–Co alloy electrodeposition as proposed in previous experiments, an important step is to choose proper substrate. For this purpose, the electrodeposition was performed on other two carbon nanomaterials: MWNT and fullerene, using the same experimental conditions as previously optimized: sweeping the potential between -0.1 and -1.3 V range for 25 scans in a bath solution containing 10 mM NiCl₂ and 10 mM CoCl₂ in 20 mM KCl. In the electrodeposition process, it is noticeable that on the forward scan, the cathodic peak characteristic for reduction of Ni²⁺ and Co²⁺ gets greater current density when MWNT is used as support comparative to fullerene and graphene (not shown). This observation indicates that the deposition of Ni–Co on the MWNT is favored when compared to the nucleation of Ni–Co on fullerene and graphene, in this order.

The electrochemical behaviors of the modified electrodes were investigated in 0.1 M KOH solution (Fig. 10). While the oxidation peak positions are similar for all electrodes ($+220$ mV), the oxidation peak currents present large variations depending on the amount and size of deposited Ni–Co nanoparticles.

The higher anodic current demonstrates that the deposition of Ni–Co on MWNT is more efficient than the formation of Ni–Co on graphene and fullerenes, which might be related to the density of active sites existent on the carbon nanotube surfaces.

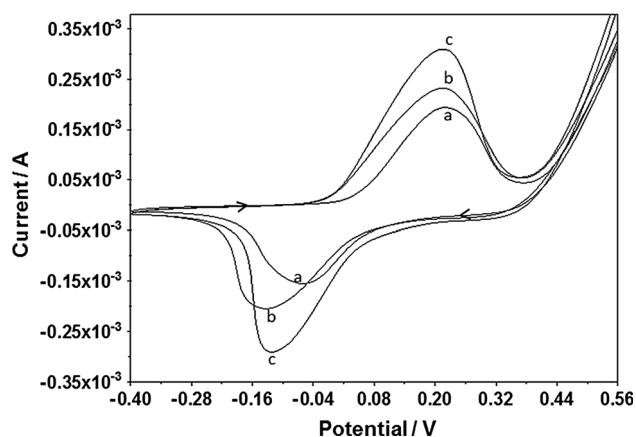


Fig. 10 Electrochemical behavior of Ni–Co deposited on **a** graphene, **b** fullerene, and **c** MWNT-based electrodes in 0.1 M KOH, scan rate 50 mV s⁻¹

The results are corroborated to SEM images taken for the three Ni–Co-modified electrodes (Fig. 11). Uniformly distributed nanoparticles can be clearly observed in all the cases, but the number of these nanoparticles increases when fullerenes are used as support rather than graphene and then more for MWNT. Moreover, the size of the Ni–Co grains is smaller when deposition is achieved on the high surface area of MWNT. It is known that small metallic particles are preferentially anchored to the high energy sites existing on the carbon surface. The density of such sites on the support influences the Ni–Co number in the resulting material. In particular, supports with higher surface areas tend to have a higher number of active sites for Ni–Co deposition. Also, the presence of defects and oxygen functional groups on MWNT, make them promising templates for efficient nucleation and growth of Ni–Co nanostructures.

Calculation of the effective surface area of the Ni–Co/MWNT and MWNT-based electrode have been performed by CV using 1 mM K₃Fe(CN)₆ containing 0.1 M KCl as a probe at different scan rates. For a reversible process, the Randles–Sevcik formula (Eq. 1) has been used [56]:

$$I_p = 2.69 \times 10^5 A n^{3/2} D^{1/2} v^{1/2} C, \quad (1)$$

where I_{pa} (A) refers to the anodic peak current; n is the number of electrons ($=1$); A (cm²) is the effective surface area of the electrode; D is diffusion coefficient of K₃[Fe(CN)₆] in 0.1 M KCl (0.673×10^{-5} cm² s⁻¹); C (mol cm⁻³) is concentration, and v (V s⁻¹) is the scan rate.

Using the slope of the I_{pa} versus $v^{1/2}$ equation, the effective area can be calculated as 0.031 cm² for MWNT and 0.123 cm² for Ni–Co/MWNT electrodes.

3.5 Comparative electrocatalytic oxidation of glucose

The electrocatalytic activities of the Ni–Co deposited on the three carbon materials have been evaluated by CV in 0.1 M KOH solution containing different concentrations of glucose (Fig. 12). When 1.2 mM glucose was added to the 0.1 M KOH electrolyte solution, notable enhancement of the anodic current could be observed, and the voltammetric response increased with raising the concentration of glucose.

In alkaline solution, NiOOH and CoOOH formed on the nanoparticle surface rapidly oxidize glucose to gluconolactone. Simultaneously, the consumption of Ni³⁺ and Co³⁺ species with the production of Ni²⁺ and Co²⁺ which are back reoxidized at electrode surface by the applied potential resulting in the increase of oxidation peak current. The response mechanism of the activated Ni–Co/carbon

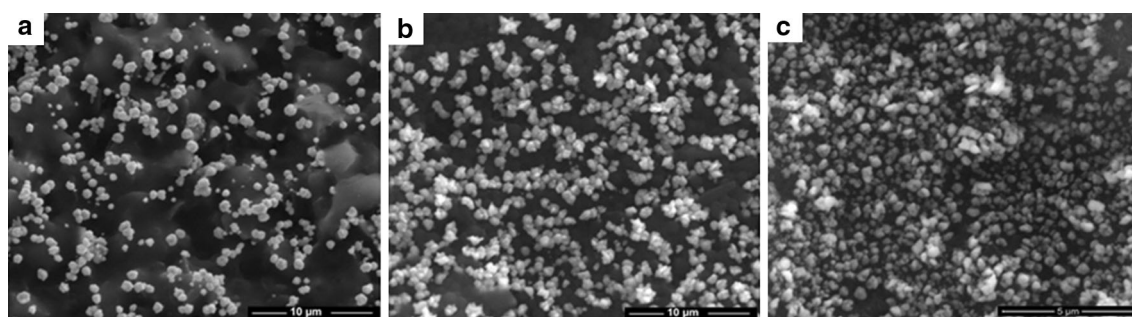
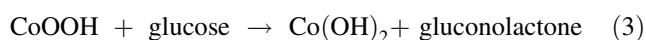
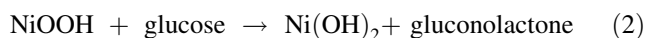


Fig. 11 SEM images of the Ni–Co nanoparticles deposited on **a** graphene, **b** fullerene, and **c** MWNT-modified electrodes in the same conditions

material to electrochemical oxidation of glucose can be simply expressed by the equations [7, 14, 37, 55, 59]:



As expected after the previous experiments, the response to glucose oxidation is highest at electrodes with Ni–Co deposited on the MWNT, confirming once again the higher density of electrodeposited Ni–Co nanoparticles on carbon nanotubes compared to Ni–Co deposited onto graphene and fullerene. The density of the particles, their smaller size corroborated to the higher specific area of nanotubes provides the highest possible electronic transfer rates for the reactions mentioned above.

On the basis of the voltammetric results, the amperometric detection of glucose at Ni–Co/carbon materials is effectively possible. Therefore, amperometric calibrations of Ni–Co/carbon material electrodes have been performed at constant potential by successive additions of glucose in 0.1 M KOH, under continuous stirring. Figure 13 shows typical amperometric responses versus time during successive additions of increasing concentration of glucose for electrodes modified by Ni–Co deposited on (a) graphene and (b) fullerene. The anodic current is proportional to the concentrations of glucose in the range of 0.005–1.5 mM for Ni–Co/graphene and 0.005–1 mM for Ni–Co/fullerene (inset of Fig. 13) deposited in similar conditions.

Our purpose is not only the construction of an electrochemical sensor for glucose but also, the evaluation and comparison of the different Ni–Co-modified electrodes. For that reason we used electrodes with Ni–Co nanoparticles deposited in different conditions on the carbon materials as previously studied, and the results are summarized in Table 1. In all the cases, the oxidation current reached a maximum steady-state value within 2–3 s upon each glucose addition. The oxidation of glucose is facilitated at numerous Ni–Co nanoparticles homogeneously deposited on the large surface area of the MWNT. The limit of detection was calculated based on the criterion of a signal-to-noise ratio of 3 and estimated to be the lowest for

Ni–Co/MWNT when applying a 0.35 V in the electrochemical sensing process.

The sensing performances of the here-developed modified electrodes compare favorably with other previously reported electrochemical glucose sensors based on the utilization of Ni or Co nanoparticles-modified electrodes as listed in Table 2. Taking Ni–Co/reduced graphene/GCE [57] as an example of an alike system, the analytical parameters for glucose detection are comparable even though the applied potential for detection is remarkably lower (of 0.3 V) in our case. The better catalytic activity and sensitivity of our Ni–Co/MWNT prove that the large surface area and porosity ensured by the substrate material has an important influence in the formation and growth of metallic nanoparticles, reflected than in the electrocatalytic activity towards glucose oxidation. Compared to other Ni-modified electrodes, the sensors described in our paper showed the advantage of lower applied potential for glucose detection which ensures a good sensitivity, a low limit of detection among and with the opportunity to minimize the interferences from other oxidizable compounds.

The low detection range obtained by these Ni–Co/carbon materials glucose sensors may allow applications to non-invasive detection of glucose in diluted blood samples using just a few ml of the sample or in other biological fluids (saliva, sweat, and urine) where glucose is too low.

The stability of Ni–Co/graphene electrode was also assessed for repetitive amperometric measurements of 65 μM glucose, applying 0.3 V, and rinsing the electrode and cell between measurements. The oxidation current displays a decrease of 7 % after 10 consecutive measurements. The same behavior was noticed also for Ni–Co/MWNT electrode, which shows a decrease of 6.7 % after 10 consecutive measurements of glucose, when applying 0.35 V. The electrode-to-electrode reproducibility was evaluated using five electrodes Ni–Co/graphene prepared independently in the same conditions. Their responses toward oxidation of 65 μM glucose were measured with a RSD of 4.5 %, indicating the reliability of the modification technique.

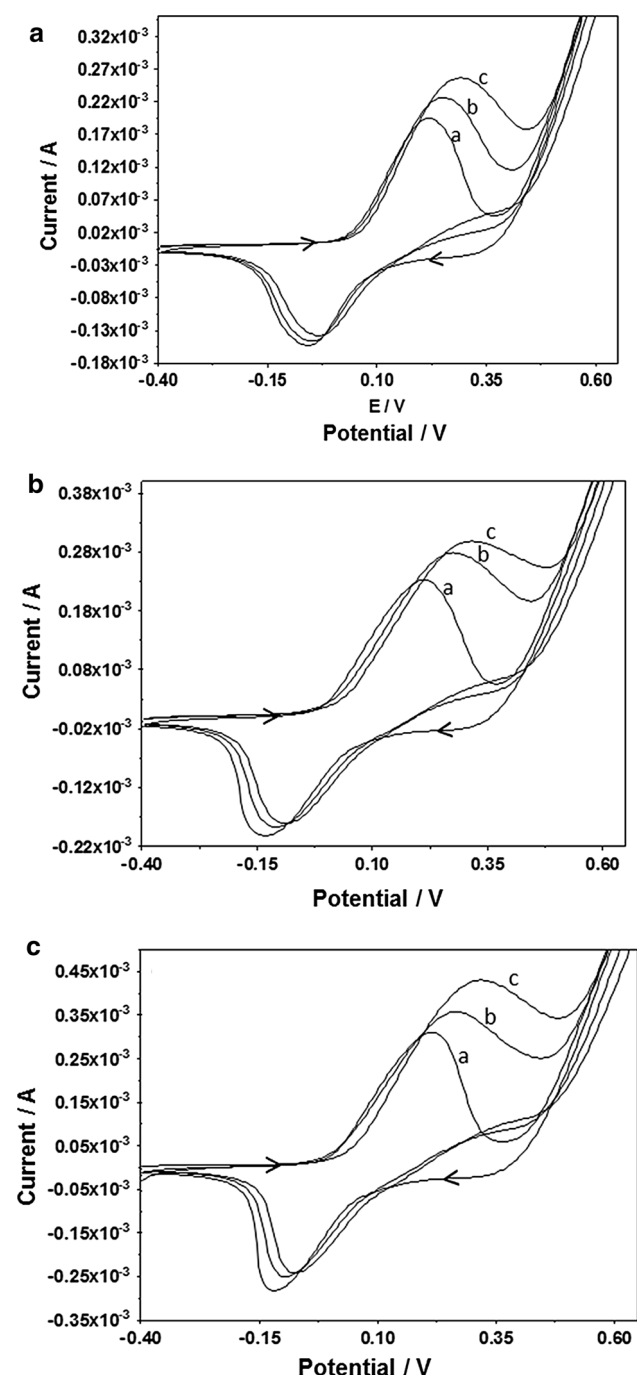


Fig. 12 Cyclic voltammetry of **a** Ni–Co/graphene, **b** Ni–Co/fullerene, and **c** Ni–Co/MWNT-modified electrodes in 0.1 M KOH in the absence (**a**) and presence of 1.2 mM (**b**) and 2.4 mM (**c**) glucose, scan rate 50 mV s^{-1}

The selectivity of a glucose sensor is related to its response for the specific analyte (glucose) in the presence of other competing species. It is known that some easily oxidative species such as ascorbic acid (AA), dopamine (DA), and uric acid (UA) usually coexist with glucose in the human serum, although in a lower concentration. Thus the electrochemical response of Ni–Co/graphene and

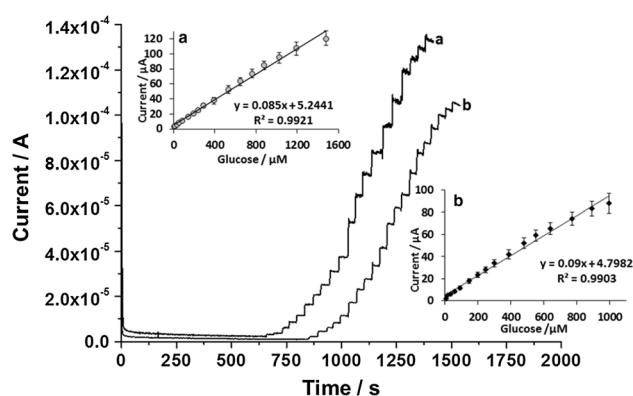


Fig. 13 Typical amperometric responses of **a** Ni–Co/graphene and **b** Ni–Co/fullerene-modified electrodes to successive additions of glucose in 0.1 M KOH, applying 0.3 V potential. *Inset*: the linear dependence of the corresponding calibration plots

Ni–Co/MWNT electrodes was also examined for the interfering species, in similar conditions, applying a 0.3 V potential.

The amperometric response of the modified electrodes was measured for an addition of $65 \mu\text{M}$ glucose followed by the successive additions of $65 \mu\text{M}$ AA, DA, and UA, respectively. Although the addition of AA induces a small rise of the current, the increase of intensity is much smaller than that for glucose (about 4 %), while DA and UA are no interfering at all in the measurement (Fig. 14), probably due to the low applied potential involved in the detection process. These results indicate that Ni–Co/carbon materials show good selectivity toward glucose and could be used as a good sensing material for highly selective and sensitive detection of glucose.

The outcomes demonstrate that the suggested method for electrodeposition of Ni–Co alloy on carbon materials is appropriate for efficient and simple construction of sensitive and selective sensor for glucose detection.

4 Conclusions

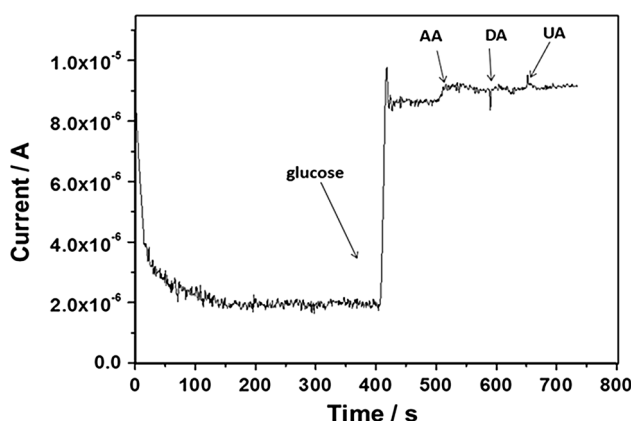
Ni–Co nanoparticles with different sizes and distributions have been comparatively electrodeposited on three carbon materials by CV. It has been shown that experimental variables such as applied potential range and cyclic number involved in the electrodeposition process affect the morphology and composition of the resulting Ni–Co nanoparticles, which is also reflected in their electrochemical activity. The electrocatalytic activity of the particles deposited on the graphene, carbon nanotubes, and fullerene was comparatively assessed by voltammetry and amperometry towards oxidation of glucose in 0.1 M KOH. The influence of the carbon material substrate was investigated: a higher density of deposited particles with smaller size

Table 1 Analytical parameters of the Ni–Co/carbon material-based electrodes for electrochemical detection of glucose at different conditions

Modified electrode	Deposition conditions	E_{app} (V)	Specific sensitivity ($\mu\text{A mM}^{-1} \text{cm}^{-2}$)	LOD (μM)	Linear range (mM)	R^2
Ni–Co/graphene	0.2 to -1.2 V; 25 scans	0.3	1163	6.1	0.005–1	0.990
Ni–Co/graphene	-0.1 to -1.3 V; 25 scans	0.3	1203	3.9	0.005–1.5	0.9921
Ni–Co/fullerene	-0.1 to -1.3 V; 25 scans	0.3	1283	3.1	0.005–1	0.9903
Ni–Co/MWNT	-0.1 to -1.3 V; 25 scans	0.3	1345	2.8	0.005–1.5	0.9914
Ni–Co/MWNT	-0.1 to -1.3 V; 25 scans	0.35	1868	1.8	0.005–2.2	0.995

Table 2 Performance of various sensors based on different electrode materials for glucose detection

Nanomaterials type	Deposition conditions	Detection potential (V)	Sensitivity ($\mu\text{A mM}^{-1} \text{cm}^{-2}$)	LOD (μM)	Linear range	Ref
Electrospun Ni nanoparticle–carbon nanofiber paste	Tedious electrospinning process	0.6	420.4	1	2 μM to 2.5 mM	[6]
CoOx·nH ₂ O–MWCNT	Electrodeposition at fix potential	0.55	162.8	2	up to 4.5 mM	[8]
Ni nanoparticles–TiO ₂ nanotube	Pulsed electrodeposition	0.6	700.2	2	0.004–4.8 mM	[50]
Ni–Co NSs/reduced graphene	Cyclic voltammetry electrodeposition	0.5	1773.61	3.79	0.01 to 2.65 mM	[57]
NiO/graphene/GCE	Pulse potential electrodeposition	0.35	15.94 $\mu\text{A mM}^{-1}$	5	0.02–2 mM	[58]
Pt/Ni–Co nanowires	Pulse electrodeposition	0.4	1125 333	1	0–0.2 mM 0.2–8 mM	[59]
3D porous Ni foam	commercially 3D Ni foam	0.45	–	2.2	0.05–7.35 mM	[60]
Ni(II)-organic coordination polymer/reduced graphene	chemical synthesis	0.45	–	0.14	0.01–8.75 mM	[61]

**Fig. 14** Influence of electroactive interferents (65 μM AA, 65 μM DA, and 65 μM UA) on the response of Ni–Co/graphene to 65 μM glucose in 0.1 M KOH, applying 0.3 V potential

when MWNT are used as support for electrodeposition facilitating thus the electrocatalytic oxidation of glucose with high sensitivity and low detection limit.

Acknowledgments This work was supported by a grant of the Romanian National Authority for Scientific Research, CNCS–UEFISCDI, project number PN-II-ID-PCCE-2011-2-0028.

References

- Zhu H, Lu XQ, Li MX, Shao YH, Zhu ZW (2009) Nonenzymatic glucose voltammetric sensor based on gold nanoparticles/carbon nanotubes/ionic liquid nanocomposite. *Talanta* 79:1446–1453
- Zhou L, Gan T, Zheng DY, Yan JJ, Hu CG, Hu SS (2012) High-density gold nanoparticles on multi-walled carbon nanotube films: a sensitive electrochemical nonenzymatic platform of glucose. *J Exp Nanosci* 7:263–273
- Baciu A, Pop A, Remes A, Manea F, Burtica G (2011) Nonenzymatic electrochemical determination of glucose on silver-doped zeolite–CNT composite electrode. *Adv Sci Eng Med* 3:13–19
- Rathod D, Dickinson C, Egan D, Dempsey E (2010) Platinum nanoparticle decoration of carbon materials with applications in non-enzymatic glucose sensing. *Sens Actuators, B* 143:547–554
- Rong LQ, Yang C, Qian QY, Xia XH (2007) Study of the nonenzymatic glucose sensor based on highly dispersed Pt nanoparticles supported on carbon nanotubes. *Talanta* 72:819–824
- Liu Y, Teng H, Hou HQ, You TY (2009) Nonenzymatic glucose sensor based on renewable electrospun Ni nanoparticle-loaded carbon nanofiber paste electrode. *Biosens Bioelectron* 24:3329–3334
- Zhu J, Jiang J, Liu J, Dinq R, Li Y, Dinq H, Feng Y, Wei G, Huang X (2011) CNT-network modified Ni nanostructured arrays for high performance non-enzymatic glucose sensors. *RSC Adv* 1:1020–1025

8. Yang J, Zhang W, Gunasekaran S (2011) A low-potential, H₂O₂-assisted electrodeposition of cobalt oxide/hydroxide nanostructures onto vertically-aligned multi-walled carbon nanotube arrays for glucose sensing. *Electrochim Acta* 56:5538–5544
9. Lu LM, Zhang XB, Shen GL, Yu RQ (2012) Seed-mediated synthesis of copper nanoparticles on carbon nanotubes and their application in nonenzymatic glucose biosensors. *Anal Chim Acta* 715:99–104
10. Chen Q, Zhang L, Chen G (2012) Facile preparation of graphene-copper nanoparticle composite by in situ chemical reduction for electrochemical sensing of carbohydrates. *Anal Chem* 84:171–178
11. Qiu R, Zhang XL, Qiao R, Li Y, Kim YI, Kang YS (2007) CuNi dendritic material: synthesis, mechanism discussion, and application as glucose sensor. *Chem Mater* 19:4174–4180
12. Li LH, Zhang WD, Ye JS (2008) Electrocatalytic oxidation of glucose at carbon nanotubes supported PtRu nanoparticles and its detection. *Electroanalysis* 20:2212–2216
13. Hui SC, Zhang J, Chen XJ, Xu HH, Ma DF, Liu YL, Tao BR (2011) Study of an amperometric glucose sensor based on PdNi/SiNW electrode. *Sens Actuators, B* 155:592–597
14. Mahshid SS, Mahshid S, Dolati A, Ghorbani M, Yang LX, Luo SL, Cai QY (2011) Template-based electrodeposition of Pt/Ni nanowires and its catalytic activity towards glucose oxidation. *Electrochim Acta* 58:551–555
15. Bai Y, Sun Y, Sun C (2008) Pt–Pb nanowire array electrode for enzyme-free glucose detection. *Biosens Bioelectron* 24:579–585
16. Marioli JM, Kuwana T (1993) Electrochemical detection of carbohydrates at nickel-copper and nickel-chromium-iron alloy electrodes. *Electroanalysis* 5:11–15
17. Luo PF, Kuwana T (1994) Nickel-titanium alloy electrode as a sensitive and stable LCEC detector for carbohydrates. *Anal Chem* 66:2775–2882
18. Day TM, Unwin PR, Macpherson JV (2007) Factors controlling the electrodeposition of metal nanoparticles on pristine single walled carbon nanotubes. *Nano Lett* 7:51–57
19. Orinakova R, Turonova A, Kladekova D, Galova M, Smith RM (2006) Recent developments in the electrodeposition of nickel and some nickel-based alloys. *J Appl Electrochem* 36:957–972
20. He Z, Chen J, Liu D, Tang H, Deng W, Kuang Y (2004) Deposition and electrocatalytic properties of platinum nanoparticles on carbon nanotubes for methanol electrooxidation. *Mater Chem Phys* 85:396–401
21. Paunovic M, Schlesinger M (1998) *Fundamentals of electrochemical deposition*. Wiley, New York
22. Harbulak EP Electroplating of nickel, cobalt, mutual alloys thereof or ternary alloys thereof with iron, US Patent 4069112, 17 Jan 1978
23. Wagner H, Scharwaechter K, Nee M Aqueous electrolytes and method for electrodepositing nickel-cobalt alloys, US Patent 4565611, 21 Jan 1986
24. Walter RJ Composition control of electrodeposited nickel-cobalt alloys, US Patent 4439284, 27 Mar 1984
25. Tang PT, Dylmer H, Moller P Electroplating method of forming platings of nickel, US Patent 6036833, 14 Mar 2000
26. Ewald R, Filke P, Heckmann M, Keinath W, Langel G, Schmidt A Method for the galvanic deposition of nickel, cobalt, nickel alloys or cobalt alloys with periodic current pulses, US Patent 6790332, 14 Sep 2004
27. Nicolas E, Merckaert L, Cathode for the electrolytic production of hydrogen and its use, US Patent 4555317, 26 Nov 1985
28. Sood AK (1986) Studies on the effect of cobalt addition to the nickel hydroxide electrode. *J Appl Electrochem* 16:274–280
29. Jovic VD, Jovic BM, Pavlovic MG (2006) Electrodeposition of Ni, Co and Ni-Co alloy powders. *Electrochim Acta* 51:5468–5477
30. Maksimovic VM, Lačnjevac UC, Stoiljkovic MM, Pavlovic MG, Jovic VD (2011) Morphology and composition of Ni–Co electrodeposited powders. *Mater Charact* 62:1173–1179
31. Rafailovic LD, Minić DM, Karnthaler HP, Wosik J, Trisovic T, Nauer GE (2010) Study of the dendritic growth of Ni–Co alloys electrodeposited on Cu substrates. *J Electrochem Soc* 157:D295–D301
32. Bai A, Hu C-C (2002) Effects of electroplating variables on the composition and morphology of nickel-cobalt deposits plated through means of cyclic voltammetry. *Electrochim Acta* 47:3447–3456
33. Lian KK, Thorpe SJ, Kirk DW (1992) The electrocatalytic activity of amorphous and crystalline Ni–Co alloys on the oxygen evolution reaction. *Electrochim Acta* 37:169–175
34. Kessler T, Triaca WE, Arvia AJ (1994) Kinetics and mechanism of the oxygen evolution reaction at oxide-coated Ni–Co amorphous alloy electrodes. *J Appl Electrochem* 24:310–315
35. Castro EB, Gervasi CA (2000) Electrodeposited Ni–Co oxide electrodes: characterization and kinetics of the oxygen evolution reaction. *Int J Hydrog Energy* 25:1163–1170
36. Lupi C, Dell’Era A, Pasquali M (2009) Nickel-cobalt electrodeposited alloys for hydrogen evolution in alkaline media. *Int J Hydrog Energy* 34:2101–2106
37. Wolfart F, Lorenzen AL, Nagata N, Vidotti M (2013) Nickel/cobalt alloys modified electrodes: synthesis, characterization and optimization of the electrocatalytic response. *Sens Actuators, B* 186:528–535
38. Arvinte A, Sesay AM, Virtanen V (2011) Carbohydrates electrocatalytic oxidation using CNT–NiCo-oxide modified electrodes. *Talanta* 84:180–186
39. Southampton Electrochemistry Group (1985) In: Kemp TJ (ed) *Instrumental methods in electrochemistry*. Ellis Horwood Ltd, Chichester
40. Vidotti M, Salvador RP, Ponzio EA, Torresi SIC (2007) Mixed Ni/Co hydroxide nanoparticles synthesized by sonochemical method. *J Nanosci Nanotechnol* 7:3221–3226
41. Elumalai P, Vasan HN, Munichandraiah N (2001) Electrochemical studies of cobalt hydroxide—an additive for nickel electrodes. *J Power Sources* 93:201–208
42. Yu S, Peng X, Cao G, Zhou M, Qiao L, Yao J, He H (2012) Ni nanoparticles decorated titania nanotube arrays as efficient nonenzymatic glucose sensor. *Electrochim Acta* 76:512–517
43. Miranda-Hernandez M, Palomar-Pardave M, Batina N, Gonzalez I (1998) Identification of different silver nucleation processes on vitreous carbon surfaces from an ammonia electrolytic bath. *J Electroanal Chem* 443:81–93
44. Scharifker B, Hills G (1983) Theoretical and experimental studies of multiple nucleation. *Electrochim Acta* 28:879–889
45. Plieth W (2008), In *Electrochemistry for Materials Science*; Plieth, W., Elsevier B.V., Amsterdam
46. Bulhoes LOS, Mascaro LH (2004) Electrochemical nucleation of lead and copper on indium-tin oxide electrodes. *J Solid State Electrochem* 8:238–243
47. Mrozek MF, Luo H, Weaver MJ (2000) Formic acid electrooxidation on platinum-group metals: is adsorbed carbon monoxide solely a catalytic poison? *Langmuir* 16:8463–8469
48. Shao M, Peles A, Shoemaker K (2011) Electrocatalysis on platinum nanoparticles: particle size effect on oxygen reduction reaction activity. *Nano Lett* 11:3714–3719
49. Inasaki T, Kobayashi S (2009) Particle size effects of gold on the kinetics of the oxygen reduction at chemically prepared Au/C catalysts. *Electrochim Acta* 54:4893–4897
50. Guerin S, Hayden BE, Pletcher D, Rendall ME, Suchsland J-P (2006) A combinatorial approach to the study of particle size effects on supported electrocatalysts: oxygen reduction on gold. *J Comb Chem* 8:679–686

51. Brenner A (1963) *Electrodeposition of alloys: principles and practice*. Academic Press, New York
52. Bai A, Hua CC (2005) Composition controlling of Co–Ni and Fe–Co alloys using pulse-reverse electroplating through means of experimental strategies. *Electrochim Acta* 50:1335–1345
53. Kamel MM (2007) Anomalous codeposition of Co–Ni: alloys from gluconate baths. *J Appl Electrochem* 37:483–489
54. Fleischmann M, Thrisk HR (1963) In: Delahay P, Tobias CW (eds) *Advances in electrochemistry and electrochemical engineering*. Wiley, New York
55. Fletcher S, Lwin T (1983) A general probabilistic model of electrochemical nucleation. *Electrochim Acta* 28:237–243
56. Bard AJ, Faulkner LR (1980) *Electrochemical methods, fundamentals and applications*. Wiley, New York, pp 218–219
57. Wang L, Lu X, Ye Y, Sun L, Song Y (2013) Nickel–cobalt nanostructures coated reduced graphene oxide nanocomposite electrode for nonenzymatic glucose biosensing. *Electrochim Acta* 114:484–493
58. Zhu XH, Jiao QF, Zhang CY, Zuo XX, Xiao X, Liang Y, Nan JM (2013) Amperometric nonenzymatic determination of glucose based on a glassy carbon electrode modified with nickel(II) oxides and graphene. *Microchim Acta* 180:477–483
59. Mahshid SS, Mahshid S, Dolati A, Ghorbani M, Yang L, Luo S, Cai Q (2013) Electrodeposition and electrocatalytic properties of Pt/Ni–Co nanowires for non-enzymatic glucose detection. *J Alloys Compd* 554:169–176
60. Lu W, Qin X, Asiri AM, Al-Youbi AO, Sun X (2013) Ni foam: a novel three-dimensional porous sensing platform for sensitive and selective nonenzymatic glucose detection. *Analyst* 138:417–420
61. Lu W, Qin X, Asiri AM, Al-Youbi AO, Sun X (2013) Facile synthesis of novel Ni(II)-based metal–organic coordination polymer nanoparticle/reduced graphene oxide nanocomposites and their application for highly sensitive and selective nonenzymatic glucose sensing. *Analyst* 138:429–433